Journal of Quantitative Spectroscopy & Radiative Transfer 112 (2011) 53–58

Contents lists available at ScienceDirect

Journal of Quantitative Spectroscopy & Radiative Transfer

journal homepage: www.elsevier.com/locate/jqsrt

Infrared absorption cross sections for acetone (propanone) in the 3 μm region

Jeremy J. Harrison*, Nicholas D.C. Allen, Peter F. Bernath

Department of Chemistry, University of York, Heslington, York YO10 5DD, United Kingdom

ARTICLE INFO

Article history:
Received 24 May 2010
Received in revised form
9 August 2010
Accepted 13 August 2010

Keywords:
Acetone
Propanone
High-resolution Fourier transform spectroscopy
Infrared absorption cross sections
Remote-sensing
Atmospheric chemistry

ABSTRACT

Infrared absorption cross sections for acetone (propanone), $CH_3C(O)CH_3$, have been determined in the 3 μm spectral region from spectra recorded using a high-resolution FTIR spectrometer (Bruker IFS 125 HR) and a multipass cell with a maximum optical path length of 19.3 m. The spectra of mixtures of acetone with dry synthetic air were recorded at 0.015 cm^{-1} resolution (calculated as 0.9/MOPD using the Bruker definition of resolution) at a number of temperatures and pressures (50–760 Torr and 195–296 K) appropriate for atmospheric conditions. Intensities were calibrated using three acetone spectra (recorded at 278, 293 and 323 K) taken from the Pacific Northwest National Laboratory (PNNL) IR database.

© 2010 Elsevier Ltd. All rights reserved.

1. Introduction

Acetone (propanone), $CH_3C(O)CH_3$, was first obtained from the destructive distillation of acetates and acetic acid, but it was not until 1832 that its molecular formula was correctly determined [1]. It is widely used as an organic solvent in lacquers, varnishes, pharmaceuticals, and cosmetics, and in numerous applications in the chemical industry as a chemical feedstock and intermediate.

Important uses are in the production of methyl methacrylate (MMA) and bisphenol A (BPA) [1]. MMA is polymerised to produce plexiglas (perspex), used principally as a substitute for glass, which is also incorporated into paints, lacquers, enamels, and coatings. BPA is used primarily to make polycarbonate plastics, which are tough and durable and commonly found in everyday items such as water bottles, food containers, bicycle helmets, compact discs, digital versatile discs, and monocle lenses.

Acetone is not only important to our modern way of life, but also to the chemistry of the atmosphere. Background mixing ratios in the free troposphere range from about 500 pptv at northern mid-latitudes to about 200 pptv at southern latitudes [2]. Mixing ratios exceeding 2 ppbv in the free troposphere have also been observed, for example in biomass burning plumes [3].

Acetone has only a negligible direct radiative forcing effect; however, like many volatile organic compounds (VOCs) it has a significant impact on air quality and is implicated in the production of tropospheric ozone, which is toxic and a strong greenhouse gas. The 2007 IPCC report [4] lists tropospheric ozone as the third most important anthropogenic factor (after methane and carbon dioxide) in driving climate change.

There is considerable uncertainty in the processes that control the atmospheric abundance of acetone. Sources of acetone include plant growth, decaying plant matter, atmospheric oxidation of organic compounds such as propane or terpenes, biomass burning, and a small contribution from anthropogenic emissions.

Recently, there has also been uncertainty in the role the oceans play in the acetone budget. Jacobs et al. [5]

* Corresponding author. Tel.: +44 1904 434589; fax: +44 1904 432516.
E-mail address: jjh506@york.ac.uk (J.J. Harrison).

0022-4073/$ - see front matter © 2010 Elsevier Ltd. All rights reserved.
doi:10.1016/j.jqsrt.2010.08.011

suggest that the oceans contribute about 28% of the atmospheric acetone from microbial and photochemical activity. Their main argument for this is the high acetone concentrations of nearly 400 ppt found in regions of the Pacific Ocean far from any terrestrial sources [6]. However, recent direct measurements of the acetone flux over the oceans have contradicted this conclusion [7], indicating that overall oceans are a large sink for acetone. An extensive global set of acetone profiles would clearly improve and constrain the acetone budget.

The sinks of acetone are primarily photolysis and reaction with OH, with a minor contribution from dry deposition. Photolytic dissociation to form the acetyl (CH_3CO) and methyl (CH_3) radicals accounts for about 50% of this, ensuring that acetone is a key part of chemistry in the atmosphere. Reactions of the acetyl radical in the upper troposphere are a major source of HO_x ($OH+HO_2$) radicals and peroxyacetyl nitrate (PAN). PAN acts as a major NO_x ($NO+NO_2$) reservoir in the free troposphere [8]. The lifetime of PAN in the troposphere increases with altitude, due to its greater thermal stability at lower temperatures, increasing from a few hours at the Earth's surface to several months at the tropopause. The relatively long lifetime in the middle and upper troposphere allows it to be transported over long distances, translating to a long-distance transport of NO_x. Nearly all tropospheric ozone results from the photolysis of NO_2, so for this reason the sources of pollutant emission may in fact be long distances from the regions of resulting elevated ozone [9].

Despite a number of ground-based [10] and airborne measurements [2,6], so far there have been no global measurements of acetone. Increasingly satellite instruments are able to directly observe VOCs, including acetone, in the atmosphere. In particular, the Atmospheric Chemistry Experiment (ACE), on board SCISAT-1, is able to detect more organic molecules in the troposphere than any other satellite instrument. In fact, the first detection of acetone using satellite infrared occultation spectroscopy was made by the ACE-FTS instrument, which sampled a biomass burning plume near the east coast of Tanzania on 8 October 2005 [3]. ACE uses a high-resolution Fourier transform spectrometer that covers the spectral region from 750 to 4400 cm^{-1} [11]. Due to this extended spectral coverage, it is possible to carry out retrievals in the strong 3 μm region, where all aliphatic hydrocarbons have their strongest-intensity modes (C–H stretch) and where there are relatively few spectral interferers. This work provides accurate spectroscopic measurements that will enable the retrieval of acetone abundances from atmospheric limb spectra recorded by ACE.

Retrievals of concentration profiles from satellite data require accurate laboratory spectroscopic measurements in the form of either line parameters or absorption cross sections. The HITRAN database [12] is a good source of such spectroscopic data; however, it does not contain acetone. Acetone data are also contained in the Pacific Northwest National Laboratory (PNNL) IR database (http://nwir.pnl.gov) [13]; however, these are not suitable for remote sensing of the upper troposphere for a number of reasons. All PNNL spectra are recorded at relatively low resolution (0.112 cm^{-1}) as mixtures with pure nitrogen gas, not synthetic air, at pressures of 760 Torr and temperatures of 278, 293, or 323 K. Despite not being suitable, these data have previously been used to retrieve acetone from ACE spectra; in particular using a micro-window centred on the prominent Q branch at 1365.5 cm^{-1} (C–H bending mode) [3].

The sparsity of good spectroscopic acetone data for remote sensing purposes can be explained by the experimental difficulties involved in taking the measurements. Acetone has a low vapour pressure (~1 Torr at 213 K and ~0.2 Torr at 197 K) [14], meaning that long optical pathlengths must be used for spectroscopic measurements in order to achieve sufficient signal to noise ratios. Until now the only available air-broadened acetone measurements suitable for remote sensing of the upper troposphere were taken by Waterfall in the 700–1780 cm^{-1} spectral region at 0.03 cm^{-1} resolution for the temperatures 224, 233, 253, 272 and 297 K [15]. The spectroscopy in this region has recently been improved and extended to lower temperatures. This will be presented in a future paper.

We have recently determined infrared absorption cross sections in the 3 μm region for air-broadened ethane [16] and propane [17]. In a similar manner, this paper presents a set of infrared absorption cross sections for air-broadened acetone between 2615 and 3300 cm^{-1}, derived from high-resolution (0.015 cm^{-1}) spectra of acetone/synthetic air recorded over a range of pressures and temperatures (50–760 Torr and 195–296 K) appropriate for atmospheric retrievals. Absorption cross sections in this less-congested spectral region will allow ACE acetone retrievals to extend to lower in the troposphere than retrievals using the Q branch at 1365.5 cm^{-1}.

2. Experimental

Experiments were performed at the Molecular Spectroscopy Facility (MSF) located at the Rutherford Appleton Laboratory, Oxfordshire, UK. The measured air-broadened acetone absorption spectra were recorded using a Bruker Optics IFS 125HR high-resolution Fourier transform spectrometer (FTS) with a calcium fluoride beam splitter, indium antimonide (InSb) detector, and an internal mid-infrared radiation source (globar). An optical filter restricted the throughput to the spectral region 2400–3500 cm^{-1}, thus reducing photon noise. The aperture diameter (2.5 mm) of the spectrometer was set so that the intensity of infrared radiation falling on the InSb detector was maximised without saturation or loss of spectral resolution. The spectrometer was set to a resolution of 0.015 cm^{-1} (calculated as 0.9/MOPD using the Bruker definition of resolution). Norton–Beer weak apodisation and Mertz phase corrections were applied to all interferograms. The FTS was evacuated to a pressure below 0.2 Pa by a turbo-molecular pump to minimise the absorbance of impurity atmospheric gases in the optical path. The FTS instrumental parameters and settings are summarised in Table 1.

The MSF short-path absorption cell (SPAC) [18] was used for all measurements. The SPAC is a multipass cell with mirrors at each end to reflect the radiation back and

forth across the length of the cell multiple times. These mirrors are fully adjustable from outside the cell, allowing the optical pathlength to be altered from 1.7 to 19.3 m in steps of 1.6 m. Transfer optics are used to transfer the radiation from the spectrometer into the cell, and from the cell onto the external InSb detector. These transfer optics are housed in chambers evacuated to pressures less than 0.02 Pa in order to minimise the absorbance of impurity atmospheric gases.

In these experiments the SPAC was operated from room temperature down to 195 K. The cylindrical sample cell is completely surrounded by an outer jacket filled with helium buffer gas. This in turn is enclosed in a jacket through which liquid nitrogen flows, entering at the top and exiting at the bottom. The desired temperature is achieved using a solenoid valve attached to the liquid-nitrogen input pipe, which is controlled by a Eurotherm unit, and a platinum resistance thermometer (PRT) measuring the temperature on the output pipe. This is all enclosed in a larger jacket kept under vacuum. This setup allows automatic temperature control for extended periods of time. The actual cell temperature was monitored by six PRTs situated at positions throughout the SPAC.

Table 1
FTS and SPAC configurations.

Source	Globar
Detector	Indium antimonide
Beam splitter	Calcium fluoride
Resolution	0.015 cm^{-1}
Aperture size	2.5 mm
Optical filter	754 (Northumbria Optical Coatings Ltd.)
Apodisation function	Norton–Beer Weak
Phase correction	Mertz
Cell windows	Sapphire
Transfer optics chamber windows	Sapphire
Mirror coatings	Gold
Pressure gauges	3 MKS-690 A Baratrons (1, 10 and 1000 Torr)
Thermometry	6 PRTs, Labfacility IEC 751 Class A

A gas-handling line was used to introduce the acetone vapour into the SPAC from a small Pyrex glass bulb. This gas line was connected to a turbomolecular vacuum pump to evacuate the line and cell between measurements. Acetone (Merck Uvasol, $\geq 99.9\%$ purity) was purified to remove dissolved air using multiple freeze-pump-thaw cycles. Dry synthetic air ('Air Zero Plus', Air Products, 20.9% $O_2 \pm 0.2\%$, $H_2O \leq 0.5$ ppm, $CH_4 \leq 0.05$ ppm, $CO+CO_2 \leq 0.1$ ppm, 99.99990% overall purity) was used 'as is' without additional purification. Sample mixtures were prepared by introducing a small amount of cold acetone vapour directly into the cell and then adding dry synthetic air. Three manufacturer-calibrated MKS-690 A Baratron capacitance manometers (full scale 1, 10 and 1000 Torr) were used during sample preparation and throughout the measurements. Thermal transpiration effects due to the positioning of the pressure gauges relative to the cell and the diameter of the connecting tubing relative to the mean free path of molecules can be safely neglected [19].

Due to the substantial decrease in the vapour pressure of acetone as it is cooled from room temperature to temperatures as low as 195 K, much care had to be taken during sample preparation to ensure that only a very small amount of acetone was transferred to the SPAC. This minimised the amount of liquid acetone condensing inside the cell, which in turn minimised the amount of time required to evacuate the cell between measurements. For this reason, the acetone sample was cooled immediately prior to preparing each sample, thus lowering the vapour pressure.

Details of pressures, temperatures, SPAC optical pathlengths, and number of scans taken for each sample are contained in Table 2. Scans of pure N_2O were also recorded at each temperature for the purposes of frequency calibration. Additionally, evacuated-cell background scans were recorded before and after the scan blocks for each sample. Ideally, an equivalent number of background scans as sample scans were measured to ensure sufficient signal to noise ratios when calculating transmittance spectra. The spectral baseline drifted slightly with time, but by using averages of backgrounds recorded before and after, most of these small drifts cancelled out.

Table 2
Summary of the sample conditions for all scans.

Acetone pressure (Torr)	Total pressure (Torr)	Temperature (K)	Pathlength[a] (m)	No. of scans[b]
0.053	50.0 ± 0.2	194.7 ± 1.0	19.31	300
0.058	75.6 ± 0.3	195.6 ± 1.0	19.31	300
0.058	100.3 ± 0.2	195.6 ± 1.0	19.31	300
0.143	49.0 ± 0.2	212.2 ± 1.0	19.31	300
0.126	109.5 ± 0.5	209.8 ± 1.0	19.31	400
0.112	263.8 ± 0.8	213.5 ± 1.0	19.31	200
0.413	204.2 ± 0.2	246.7 ± 0.5	8.11	250
0.369	400.6 ± 0.5	247.0 ± 0.5	8.11	260
0.384	600.1 ± 0.5	246.9 ± 0.5	8.11	250
0.681	370.0 ± 0.2	268.7 ± 0.3	4.91	250
0.679	600.8 ± 0.4	268.7 ± 0.3	4.91	250
0.997	758.9 ± 0.4	296.0 ± 0.3	3.31	250

[a] The error in the optical pathlength is estimated to be $\pm 0.2\%$ at room temperature.
[b] Note that each sample requires the measurement of a similar number of background scans taken with the same spectrometer settings. One scan takes about 33 s.

Care was taken to prevent impurities inside the cell at low temperatures using high purity gases and pumping out the gas line before the preparation of sample mixtures. Despite this, however, very weak absorption lines of water were observed in the sample scans.

The temperatures and pressures of the samples in the SPAC were logged every few seconds. The variations in these quantities were used to estimate their experimental uncertainties (see Table 2), which range from 0.1% at room temperature to 0.5% at the lowest temperatures. The tabulated acetone partial pressures are somewhat unreliable because they reflect the initial pressure before the addition of synthetic air. This addition resulted in a small increase in the temperature, which in turn slightly increased the acetone partial pressure. This has made it necessary to normalise the measurements against an accurate intensity standard. In this work we have chosen to use acetone spectra from the PNNL IR database. This is discussed further in Section 3.

The error in the SPAC optical pathlengths (see Table 2) at room temperature is estimated to be $\pm 0.2\%$. The pathlength changes slightly as the cell is cooled because the mirrors and optical components change position as they contract. Any systematic error in the pathlength will be accounted for by normalising against acetone spectra from the PNNL IR database.

The photometric uncertainty is estimated to be 1–2%, and the overall uncertainties in the absorption cross sections reported in this work are estimated to be 3%.

3. Results and discussion

Transmission spectra were calculated by dividing averaged single-channel sample scans by appropriate averaged single-channel background scans. A further small correction was necessary to ensure that the baseline extended to 100% transmittance outside the absorption band. Spectral frequencies were calibrated using pure N_2O spectra, which were recorded during the experimental run. The accurate positions of isolated N_2O absorption lines in the 3 μm region were determined from the HITRAN database [12]. Any weak absorption lines of water in the spectra were removed by hand.

Due to the temperature sensitivity of the acetone vapour pressure at low temperatures, the amount of absorber in the SPAC optical pathlength was relatively uncertain. For this reason, the *y*-axes of the cross sections derived in this work were calibrated using acetone spectra from the PNNL IR database. Each PNNL spectrum is a composite of multiple pathlength–concentration burdens, and great care has been taken to ensure that sample concentrations have been determined accurately. This calibration also relies on the fact that band intensities for isolated bands comprising primarily fundamentals are essentially independent of temperature [16].

Spectral absorption cross sections, $\sigma(\upsilon,P_{air},T)$, with units $cm^2\ molecule^{-1}$, were calculated by the equation

$$\sigma(\upsilon,P_{air},T) = -\xi \frac{10^4 k_B T}{Pl} \ln \tau(\upsilon,P_{air},T) \quad (1)$$

where $\tau(\upsilon,P_{air},T)$ is the transmittance at wavenumber υ (cm^{-1}), temperature T (K) and synthetic air pressure P_{air}, P is the pressure of the absorbing gas (Pa), l the optical pathlength (m), k_B the Boltzmann constant ($=1.3806504\times10^{-23}\ J\ K^{-1}$), and ξ the factor required to satisfy the following normalisation requirement:

$$\int_{2615\ cm^{-1}}^{3300\ cm^{-1}} \sigma(\upsilon,P_{air},T) = 8.105\times10^{-18}\ cm\ molecule^{-1}\ (\pm 0.3\%) \quad (2)$$

The value on the right hand side of Eq. (2) is the average integrated band strength of the three acetone PNNL spectra (recorded at 278, 293, and 323 K) between 2615 and 3300 cm^{-1}, converted from PNNL units using the factor $k_B\times296\times\ln10\times10^4/0.101325$. The uncertainty in parentheses represents the spread from the mean of the three integrated band intensities. Following the application of Eq. (2), the cross sections were re-baselined to agree with the baseline of the PNNL spectra and then normalised for a final time.

A selection of acetone absorption cross sections is given in Figs. 1 and 2. In the first figure is a plot of three cross sections at ~195 K and 50.0, 75.6 and 100.3 Torr.

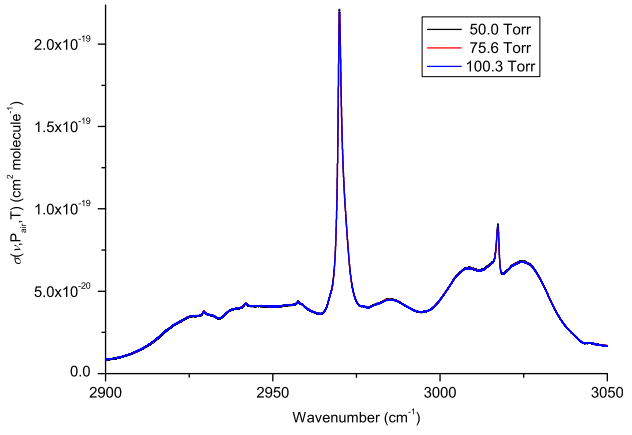

Fig. 1. Acetone absorption cross sections at ~195 K and 50.0, 75.6 and 100.3 Torr. The addition of synthetic air has very little effect on the broad acetone structure.

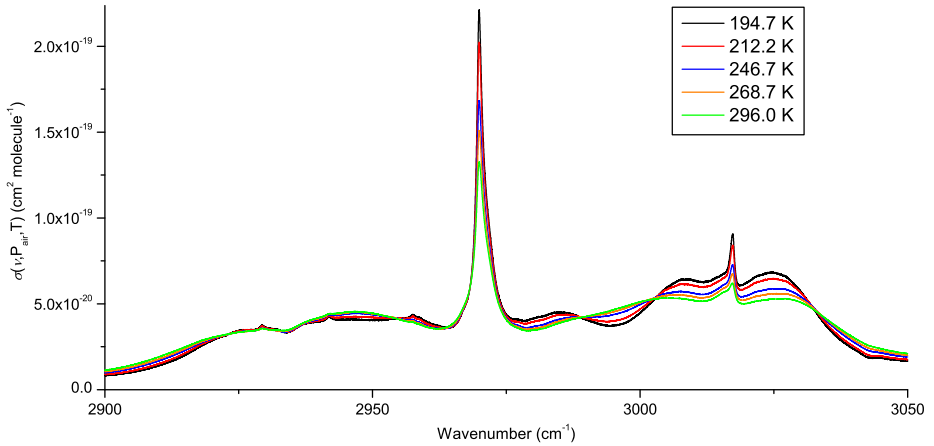

Fig. 2. Acetone absorption cross sections at five temperatures (194.7, 212.2, 246.7, 268.7 and 296.0 K) corresponding to the lowest broadening pressures available in the data set for each temperature block (refer to Table 2 for the corresponding pressures). A sharpening of the structure is observed with decrease in temperature.

The structure in these cross sections is broad and additional synthetic air has only a small effect on this broadening. At all temperatures, a small amount of sharpening of the Q branches can be observed with decrease in air pressure over large pressure ranges.

In the second figure are plotted acetone absorption cross sections at five temperatures (194.7, 212.2, 246.7, 268.7 and 296.0 K) corresponding to the lowest broadening pressures available in the data set for each temperature block (refer to Table 2 for the corresponding pressures). A sharpening of the structure is readily observed as the temperature decreases.

All the spectral absorption cross sections corresponding to the experimental conditions in Table 2 are available electronically upon request from the authors.

4. Conclusions

High-resolution infrared absorption cross sections for acetone (between 2615 and 3300 cm^{-1}) have been determined with an estimated uncertainty of 3%. Spectra were recorded for mixtures of acetone with dry synthetic air at 0.015 cm^{-1} resolution using a range of temperatures and pressures appropriate for atmospheric conditions and a multipass cell with a maximum optical path length of 19.3 m. Intensities were calibrated against three acetone spectra (recorded at 278, 293 and 323 K) taken from the PNNL IR database. These cross sections will be used in the development of an ACE acetone data product, and in particular will allow retrievals from lower in the troposphere than possible using the Q branch at 1365.5 cm^{-1}, which is located in a particularly congested spectral region.

Acknowledgements

The authors wish to thank the Natural Environment Research Council (NERC) for supporting J.J. Harrison through grant NE/F002041/1, and N.D.C. Allen through the National Centre for Earth Observation (NCEO), and for access to the Molecular Spectroscopy Facility (MSF) at the Rutherford Appleton Laboratory (RAL). R.G. Williams is thanked for providing technical support at the RAL.

References

[1] Myers RL. The 100 most important chemical compounds: a reference guide. Westport, Connecticut, USA: Greenwood Press; 2007.
[2] Singh HB, Kanakidou M, Crutzen PJ, Jacob DJ. High concentrations and photochemical fate of oxygenated hydrocarbons in the global troposphere. Nature 1995;378:50–4.
[3] Coheur P-F, Herbin H, Clerbaux C, Hurtmans D, Wespes C, Carleer M, et al. ACE-FTS observation of a young biomass burning plume: first reported measurements of C_2H_4, C_3H_6O, H_2CO and PAN by infrared occultation from space. Atmos Chem Phys 2007;7:5437–46, doi:10.5194/acp-7-5437-2007.
[4] IPCC. Climate change 2007: the physical science basis. In: Solomon S, Qin D, Manning M, Chen Z, Marquis M, Averyt KB, Tignor M, Miller HL, editors. Contribution of working group i to the fourth assessment report of the intergovernmental panel on climate change. Cambridge, United Kingdom and New York, NY, USA: Cambridge University Press; 2007. See 〈http://www.ipcc.ch/〉.
[5] Jacob DJ, Field BD, Jin EM, Bey I, Li Q, Logan JA, et al. Atmospheric budget of acetone. J Geophys Res 2002;107(D10):4100, doi:10.1029/2001JD000694.
[6] Singh HB, O'Hara D, Herlth D, Sachse W, Blake DR, Bradshaw JD, et al. Acetone in the atmosphere: distribution, sources, and sinks. J Geophys Res 1994;99(D1):1805–19.
[7] Marandino CA, De Bruyn WJ, Miller SD, Prather MJ, Saltzman ES. Oceanic uptake and the global atmospheric acetone budget. Geophys Res Lett 2005;32:L15806, doi:10.1029/2005GL023285.
[8] Singh HB, Hanst PL. Peroxyacetyl nitrate (PAN) in the unpolluted atmosphere: an important reservoir for nitrogen oxides. Geophys Res Lett 1981;8(8):941–4.
[9] Gupta ML, Cicerone RJ, Blake DR, Rowland FS, ISA Isaksen. Global atmospheric distributions and source strengths of light hydrocarbons and tetrachloroethene. J Geophys Res 1998;103(D21): 28219–35.
[10] Lewis AC, Hopkins JR, Carpenter LJ, Stanton J, Read KA, Pilling MJ. Sources and sinks of acetone, methanol, and acetaldehyde in North Atlantic marine air. Atmos Chem Phys 2005;5:1963–74, doi:10.5194/acp-5-1963-2005.
[11] Bernath PF, McElroy CT, Abrams MC, Boone CD, Butler M, Camy-Peyret C, et al. Atmospheric chemistry experiment (ace): mission overview. Geophys Res Lett 2005;32(L15S01), doi:10.1029/2005GL022386.
[12] Rothman LS, Gordon IE, Barbe A, Benner DC, Bernath PF, Birk M, et al. The HITRAN 2008 molecular spectroscopic database. J Quant Spectrosc Radiat Transf 2009;110:533–72.

[13] Sharpe S, Johnson T, Sams R, Chu P, Rhoderick G, Johnson P. Gas-phase databases for quantitative infrared spectroscopy. Appl Spectrosc 2004;58(12):1452–61.
[14] Yaws Carl L. Chemical Properties Handbook. McGraw-Hill; 1999.
[15] Waterfall, AM. Measurement of organic compounds in the upper troposphere using infrared remote sensing. DPhil thesis, University of Oxford, 2004.
[16] Harrison JJ, Allen NDC, Bernath PF. Infrared absorption cross sections for ethane (C_2H_6) in the 3 μm region. J Quant Spectrosc Radiat Transf 2010;111:357–63, doi:10.1016/j.jqsrt.2009.09.010.
[17] Harrison JJ, Bernath PF. Infrared absorption cross sections for propane (C_3H_8) in the 3 μm region. J Quant Spectrosc Radiat Transf 2010;111:1282–8, doi:10.1016/j.jqsrt.2009.11.027.
[18] Paynter DJ, Ptashnik IV, Shine KP, Smith KM, McPheat R, Williams RG. Laboratory measurements of the water vapor continuum in the 1200–8000 cm^{-1} region between 293 and 351 K. J Geophys Res 2009;114:D21301, doi:10.1029/2008JD011355.
[19] Takaishi T, Sensui Y. Thermal transpiration effect of hydrogen, rare gases and methane. Trans Faraday Soc 1963;59: 2503–14.